AJNR

Comparison of gradient-recalled-echo and T2-weighted spin-echo pulse sequences in intramedullary spinal lesions.

B H Katz, R M Quencer and R S Hinks

AJNR Am J Neuroradiol 1989, 10 (4) 815-822
http://www.ajnr.org/content/10/4/815

Comparison of Gradient-Recalled-Echo and T2-Weighted Spin-Echo Pulse Sequences in Intramedullary Spinal Lesions

Barry H. Katz[1]
Robert M. Quencer[1]
R. Scott Hinks[2]

Nineteen consecutive patients with spinal intramedullary lesions were studied on a 1.5-T system to compare the quality of T2-weighted spin-echo and gradient-recalled-echo (GRE) pulse sequences. Direct comparisons were made in the sagittal and/or axial planes. Twenty-four studies were performed in the 19 patients. The gradient echoes were usually performed at 300/14 (TR/TE) with a flip angle of 10°. Although no significant diagnostic differences were noted in the sagittal plane, there was a distinct anatomic advantage for GRE imaging over spin-echo imaging in the axial plane. This is believed to be the result of CSF time-of-flight effects in the slice-select direction, which are not compensated for by flow-compensating gradients on the spin-echo images, but which are insignificant in the GRE sequence used in this study. Pathology was seen equally well or better on GRE in 79% (19/24) of the sequences. In the other five cases, the spin-echo image showed a brighter intramedullary signal than that seen on GRE, although GRE showed the lesion in all cases.

Our results indicate that properly optimized GRE imaging on a high-field-strength system can replace spin-echo imaging in the spine when intramedullary disease is suspected and that the benefits of GRE are most striking in the axial plane.

MR imaging has become a widely accepted technique in the evaluation of diseases affecting the spine and spinal cord. For the evaluation of intramedullary lesions, T2-weighted spin-echo (SE) images have been widely used; however, the long scanning time required for SE has several disadvantages, including the potential for increased patient motion and CSF motion artifacts. Recently, gradient-recalled echoes (GREs) have been used as a fast scanning technique to decrease scanning time while achieving a T2 "myelogram" effect [1–6]. Its primary application in the spine has been in the evaluation of extradural disease [6–8]. Our prospective study was carried out to investigate the efficacy of GRE in evaluating intramedullary lesions by directly comparing GRE and SE findings in both the axial and sagittal planes.

Subjects and Methods

We evaluated prospectively the MR scans of 19 consecutive patients with intramedullary spinal cord lesions by a qualitative comparison of the T2-weighted SE and GRE images. All comparisons were made in the same projection (i.e., axial and/or sagittal planes). The scans were obtained with a 1.5-T superconducting magnet* with surface-coil imaging, and all sequences were performed during the same examination period. The patient group comprised 10 men and nine women 11–75 years old (mean, 45.1 years).

The GRE sequences, 250–300/14 (TR/TE), used a TR of 300 msec in 19 of 24 sequences. The flip angle averaged 9.6°; 21 of 24 sequences used a flip angle of 10.0° ± 0.5°. The gradient echoes were done with 5- to 6-mm contiguous slices, no interslice gap, four repetitions, and a 192 × 256 acquisition matrix. All scans were obtained with a multislice technique acquiring eight slices per sequence. The average scan time for GRE sequences was 3.8 min. SE sequences, 2000–2500/80–100/2 (TR range/TE range/excitations), were

Received July 8, 1988; revision requested August 24, 1988; revision received November 11, 1988; accepted December 13, 1988.

[1] Department of Radiology, University of Miami School of Medicine/Jackson Memorial Medical Center, Miami, FL 33101. Address reprint requests to R. M. Quencer, University of Miami M.R.I. Center, 1115 N.W. 14th St. (R-308), Miami, FL 33136.

[2] Picker International Clinical Science Research Center, Highland Heights, OH 44132.

AJNR **10:815–822, July/August 1989**
0195–6108/89/1004–0815

* Picker International, Inc., Highland Heights, OH.

done with the motion-artifact suppression technique (MAST) [9, 10]. Five- to six-millimeter contiguous slices and a 192 × 256 acquisition matrix were used.

Only pulse sequences that had both an SE and a GRE image in the same plane were included in this study. The evaluation and comparison of the GRE and SE images were based on both delineation of normal anatomic structures in the sac and cord as well as appreciation of character and extent of disease. In this comparative study, equality or superiority of image quality was recorded. The distribution of studies in terms of spinal level was cervical, 11; thoracic, seven; and lumbar, one. Of the 19 patients studied, GRE and SE were compared in a single plane in 14 and in two planes in five.

Results

The spinal level, axis of examination, and diagnosis in each patient are outlined in Table 1. Comparison of thecal sac and cord anatomy is shown in Table 2. There was a striking disparity in favor of GRE in terms of visualizing normal anatomy in the axial plane. In seven of eight (88%) patients, axial GRE was superior to axial SE (Figs. 1–4). The studies were judged to be equal in one. In the seven cases in which GRE was superior, there was a sharp, well-defined interface between the intramedullary lesion and normal cord and between the cord and CSF. Five of these seven patients were imaged in the cervical spine; the other studies were thoracic. On SE images, the lesion/cord and cord/CSF interfaces were indistinct. In the sagittal sequences, only one (6.3%) of 16 cases had a better SE study in terms of quality of anatomy. In 69% (11/16), SE and GRE were believed to be equivalent (Figs. 3C and 3D), while GRE was superior in 25% (4/16). Thus, anatomically, GRE was at least equal to SE of the spine in the sagittal plane (Figs. 3C, 3D, and 5–7).

Concerning definition of pathology, 50% (12/24) of the total sequences showed no difference in ease of visualization of spinal cord disease. GRE was superior in 29% (7/24), while SE was better in 21% (5/24). However, in all cases in which the lesion was better visualized on SE, it was also seen on the GRE sequences. The lesion simply was "brighter" on SE in these instances. In addition, in a patient with recurrent intramedullary hemorrhage (Fig. 7, case 16), the gradient echo was sensitive in depicting hemorrhage secondary to the high magnetic susceptibility of blood. The T2 shortening effects of hemosiderin were seen equally well on the SE image.

TABLE 1: Gradient-Recalled-Echo and T2-Weighted Spin-Echo Imaging of Intramedullary Spinal Lesions: Summary of Patients and Scanning Locations and Projections

Study Level/ Case No.	Imaging Plane	Diagnosis
Cervical		
1	Sagittal	Spondylosis with gliosis/edema
2	Sagittal	Spondylosis with cord gliosis/ edema
3	Axial	Neurofibromatosis with glioma
4	Axial	Multiple sclerosis plaques
5	Sagittal and axial	Multiple sclerosis plaques
6	Sagittal	Multiple sclerosis plaques
7	Axial	Infarct vs multiple sclerosis
8	Sagittal	Intramedullary cysts or myelomalacia secondary to trauma
9	Sagittal and axial	Myelomalacia vs intramedullary cyst secondary to trauma
10	Sagittal	Traumatic intramedullary cyst
11	Sagittal and axial	Myelitis in AIDS patient
Thoracic		
12	Sagittal and axial	Neurofibromatosis with hamartoma/glioma
13	Sagittal	Fracture/dislocation with nonpulsatile intramedullary cyst
14	Sagittal	Intramedullary cyst secondary to trauma
15	Sagittal and axial	Intramedullary lung metastasis with syringohydromyelia
16	Sagittal	Intramedullary hemorrhage secondary to occult arteriovenous malformation
17	Sagittal	Hemorrhagic cord lesion—arteriovenous malformation vs hemangioblastoma
18	Sagittal	Cord edema/gliosis secondary to compression from extradural metastases
Lumbar		
19	Sagittal	Diastematomyelia with hydromyelia in tethered cord

Discussion

T2-weighted SE imaging has become the method of choice in the evaluation of intramedullary spinal cord lesions. The excellent sensitivity of this pulse sequence has allowed spinal intramedullary lesions to be diagnosed even in the face of a normal-sized cord. However, several problems are evident with this technique as a result of the long imaging times required (typically 10–15 min) and the phase errors and artifacts [11–14] that are present on long TR/long TE pulse sequences. GRE pulse sequences can generate "T2-like" images without the CSF flow-induced artifacts in relatively short periods of time. Because such sequences have been shown to be useful in the detection of disk disease in the cervical and lumbar spine [6–8], we sought to determine whether GRE studies were equally helpful in spinal cord disease and whether such an examination could replace SE imaging. Evaluation of spinal cord disease using the GRE parameters described in this article at high field strengths has not been previously reported.

Enzmann and Rubin [15] concluded that a short TR GRE (gradient-recalled acquisition in the steady state, GRASS)

TABLE 2: Comparison of Gradient-Recalled-Echo (GRE) and Spin-Echo (SE) Imaging of Spinal Cord and Thecal Sac Anatomy

Study Rating	No. of Studies	
	Sagittal Plane	Axial Plane
GRE superior to SE	4	7
SE superior to GRE	1	0
GRE and SE equal	11	1
Total	16	8

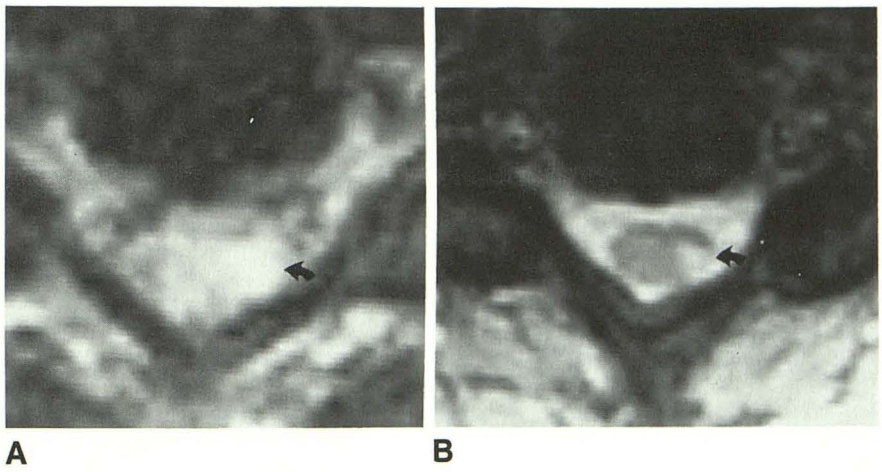

Fig. 1.—Case 7: 75-year-old man with 2-year progressive myelopathy and left-sided weakness.
***A*, Axial SE image (2000/100) barely shows lesion at C4–C5 level in left side of cord (*arrow*). Lesion is poorly defined and blends imperceptibly with cord and CSF.**
***B*, GRE image (300/14, 10° flip angle) through same area clearly depicts sharply defined lesion (*arrow*) and its relationship to remainder of cord and surrounding CSF.**

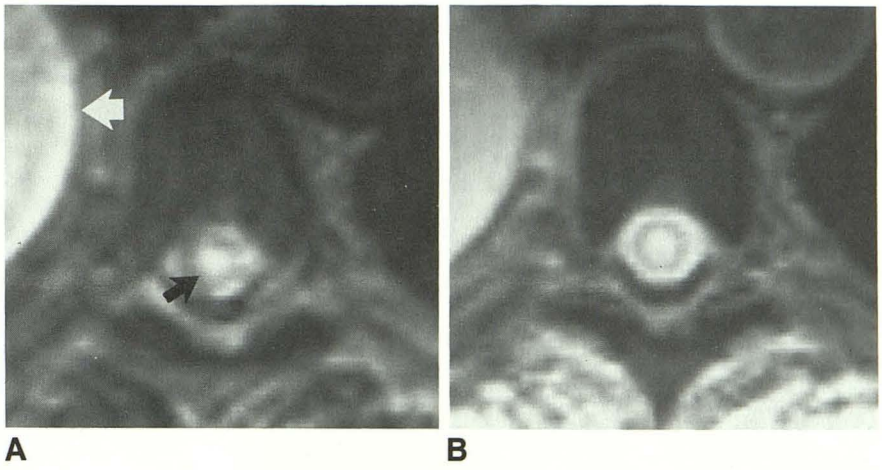

Fig. 2.—Case 15: Intramedullary metastases with syringomyelia of thoracic cord.
***A*, Axial SE image (2000/100) at T8 clearly shows intramedullary lesion (*black arrow*), but lesion/cord and cord/CSF interfaces are poorly defined. Note right lung mass (*white arrow*).**
***B*, GRE image (300/14, 10° flip angle) through same level illustrates superior anatomic delineation compared with SE. Lesion is seen equally well on both images, but GRE is judged overall to be superior to SE.**

sequence is less effective than a CSF-gated T2-weighted SE sequence in the evaluation of spinal lesions, especially in the sagittal plane. The TRs used in their study (22–50 msec), however, were considerably shorter than those used in our series (300 msec). The use of the longer TR in our study results in improved signal-to-noise and reduced artifacts as described below.

The classical GRE pulse sequence (also known as GRASS, field-echo, gradient-echo, or limited flip-angle imaging) is a short TR/TE sequence with a partial flip angle. Optimization of contrast resolution, spatial resolution, and signal-to-noise ratio (SNR) in this technique is critical for lesion detection. The magnitude of the flip angle chosen appears to be the most important parameter in terms of producing proper image contrast [2, 3, 6, 7, 15, 16]. Although the reduced flip angle is most responsible for the relatively low SNR in GRE (less transverse magnetization produces less signal), a flip angle of 10° or less is best to achieve a T2-like effect with excellent contrast [6, 7, 15]. This is primarily because the reduced flip angle reduces or eliminates the T1 weighting, which normally competes with T2 weighting and decreases contrast.

The signal in GRE imaging is based on the following equation:

$$S = \frac{(1 - e^{-TR/T1}) \times M_o \times \sin \phi}{1 - (e^{-TR/T1} \times e^{-TR/T2^*}) - \cos(\phi) \times (e^{-TR/T1} - e^{-TR/T2^*})} \quad (1)$$

where M_o is the proton density and ϕ is the flip angle [1, 4, 6]. This simplifies to:

$$S = \frac{M_o \times \sin \phi \times (1 - e^{-TR/T1}) \times e^{-TE/T2^*}}{1 - \cos \phi \times e^{-TR/T1}} \quad (2)$$

when $TR \gg T2^*$, as it is in our sequence since $e^{-TE/T2^*}$ approaches zero. By decreasing the flip angle toward zero (i.e., 10°), cos ϕ approaches one and the equation reduces to:

$$S = \frac{M_o \times \sin \phi \times (1 - e^{-TR/T1}) \times e^{-TE/T2^*}}{(1 - e^{-TR/T1})} \quad (3)$$

The terms $(1 - e^{-TR/T1})$ cancel and we are left with:

$$S = M_o \times \sin \phi \times e^{-TE/T2^*} \quad (4)$$

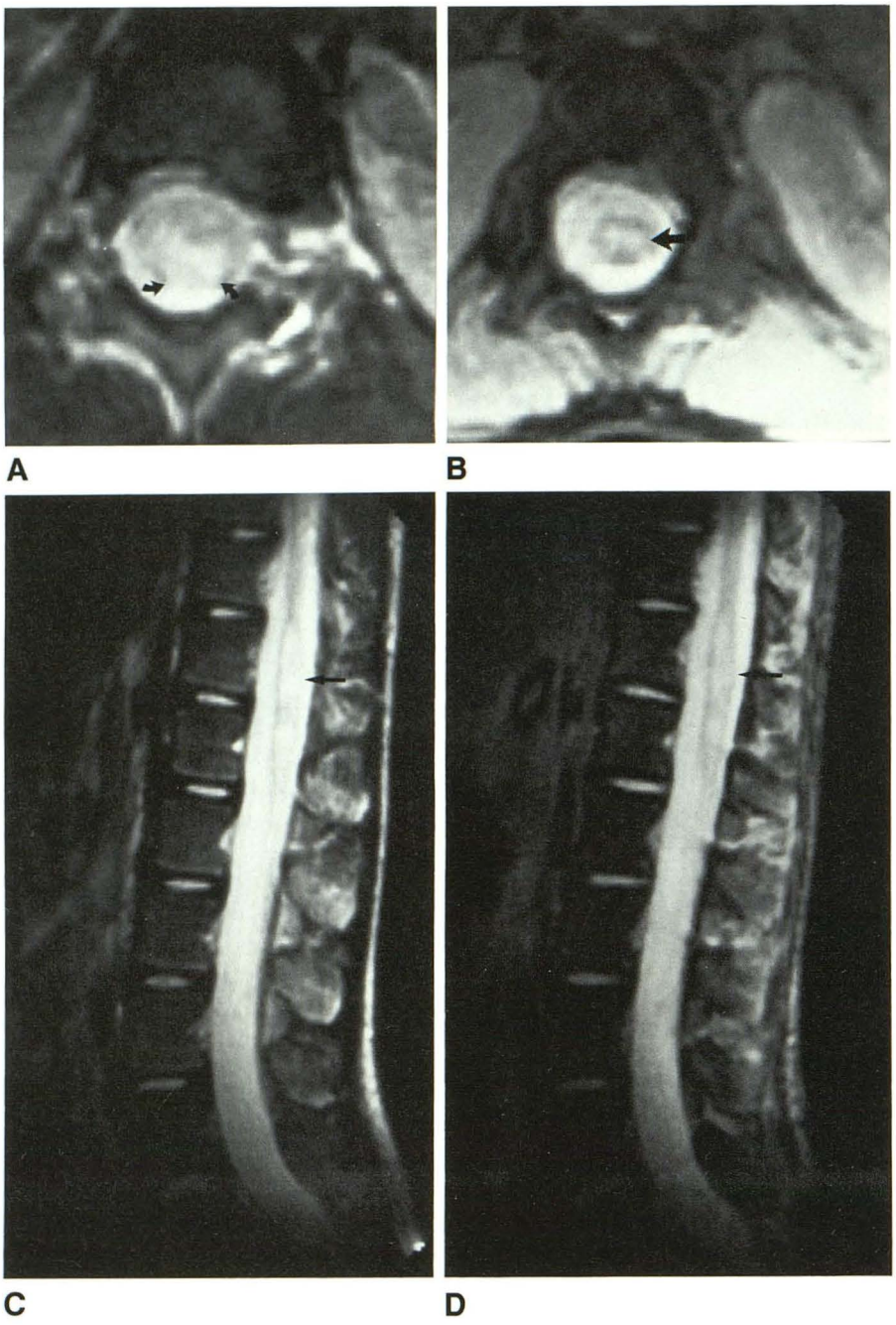

Fig. 3.—Case 12: 11-year-old patient with neurofibromatosis and presumed hamartoma/glioma in distal cord.

***A*, SE image (2100/80) at T12 shows high signal within canal, but it is not certain whether abnormality (*arrows*) lies within cord. CSF/cord interface is not identified.**

***B*, GRE image (300/14, 10° flip angle) at same level shows anatomy and intrinsic cord lesion well (*arrow*).**

***C* and *D*, SE (*C*) and GRE (*D*) sagittal images through distal cord and conus show increased intrinsic cord signal (*arrows*) without evidence of abnormal cord enlargement. These two images are essentially identical in quality.**

As seen in equation 4, the signal strength and contrast are dependent on proton density (larger M_o yields brighter signal) and T2* (longer T2* yields brighter signal). At the short TE used in this study (14 msec), the signal is primarily determined by proton density with a lesser contribution from T2*. T2* is a time constant that describes a signal decay from several sources including T2, static field inhomogeneity, chemical shift, and magnetic susceptibility. In routine T2-weighted SE imaging, the terms other than T2 cancel owing to the refocusing effect of the 180° RF pulse.

The differences between short TR and long TR GRE sequences can be explained as follows. The use of a short TR leads to the buildup of a "steady state" of transverse magnetization. This occurs when the sequence is repeated so rapidly that the signal does not fully decay from one excitation to the next and is refocused by successive RF pulses. This effect is seen in the dependence of the signal on $e^{-TR/T2^*}$, as shown in equation 1 above. The pulsatile flow of CSF alters this steady state in two ways. First, phase errors caused by flow effects alter the steady-state signal when unsaturated protons enter a given slice and the fully magnetized protons exit the slice. Both effects result in flow artifacts in the phase-encoding direction and decrease diagnostic value. With the relatively long TR used in this study, the buildup of steady-

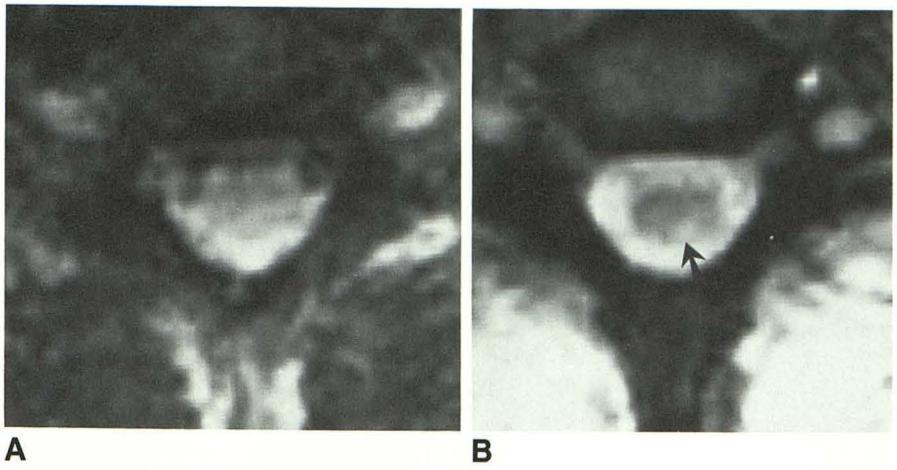

Fig. 4.—Case 4: Multiple sclerosis plaques in cervical cord.

***A*, SE image (2200/100) at C6–C7 level does not clearly identify cervical cord lesion. Ventrally, separation between cord and CSF is poor.**

***B*, GRE image (300/14) at same level shows cord lesion (*arrow*). Anatomic resolution with GRE is superior to that with SE.**

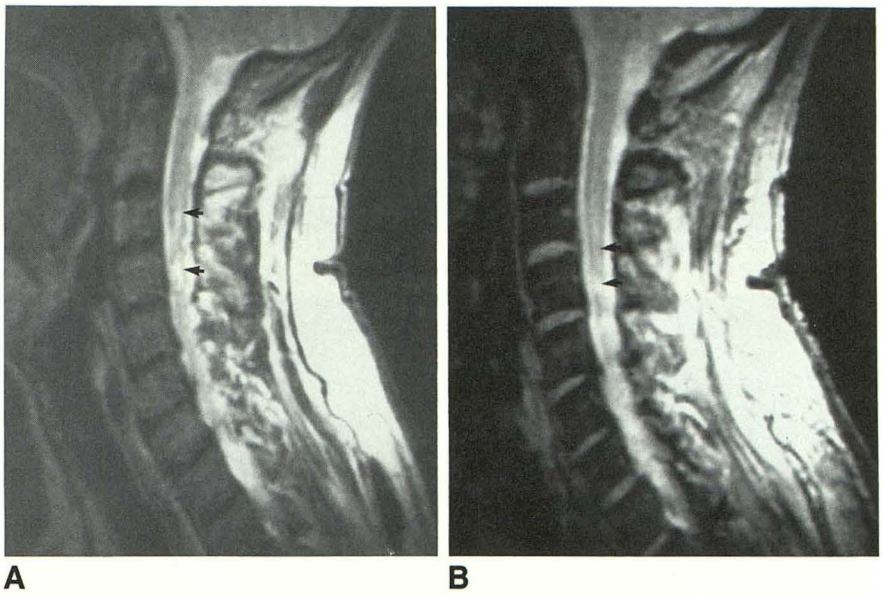

Fig. 5.—Case 2: Cord edema/gliosis secondary to extradural compression from spondylosis.

***A*, SE image (2000/100) shows lesion (*arrows*) in cord at C3 and C4. Note spondylitic changes.**

***B*, Sagittal GRE image (300/14, 10° flip angle) shows better definition of intervertebral disks and anterior subarachnoid space. Pathology (*arrows*) and overall definition of spinal cord are nearly equivalent.**

state transverse magnetization is effectively eliminated. Phase errors caused by flow are minimal because the TE is so short that only small phase shifts can accumulate. In addition, time-of-flight effects are eliminated because the reduced flip angle removes the T1 dependence, and there is likewise no steady-state magnetization to be disrupted by flow through the plane. These factors result in a GRE sequence that is relatively insensitive to CSF flow effects and has improved image quality and lesion detectability.

The inherently low SNR usually seen with GRE was compensated in our study by the following four considerations. (1) The high-field-strength magnet improves SNR in approximately a linear relationship compared with a lower-field-strength system [17]. (2) The use of a 192 × 256 acquisition matrix yields adequate spatial resolution with a 15% increase in SNR compared with a 256 × 256 data matrix. Also, the use of this matrix reduces the scan time such that four repetitions can be used with a relatively short examination (4 min). (3) By increasing TR from 25–50 msec to 300 msec, the SNR improves, allowing better visualization of cord lesions. Short TR sequences (25–30 msec) are generally adequate for extradural disease but do not offer adequate signal-to-noise to effectively evaluate intramedullary disease [6, 7, 15]. (4) A short TE also improves the SNR, just as it does in routine SE sequences. Other investigators have used similar TEs in their GRE imaging [6, 7, 15, 16]. The use of a short TE minimizes the effect of T2* on image contrast. Thus, our GRE images are primarily proton-density weighted with a small contribution from T2*. We can visualize the central gray matter including the dorsal and ventral horns in the axial plane (Fig. 8). Intramedullary lesions such as tumors, cysts, or multiple sclerosis disrupt these anatomic details (Figs. 1, 2, 3A, 3B, and 4) and produce patchy or well-defined, rounded lesions. Given the excellent anatomic depiction of spinal anatomy with GRE, especially in the axial plane, a variety of spinal cord lesions can be detected easily. In fact, in our three patients with multiple sclerosis plaques, both the anatomy and pathology were better visualized on GRE than on SE images. Given similar SNRs, one would expect that lesions that are visualized on SE would also be expected to be seen

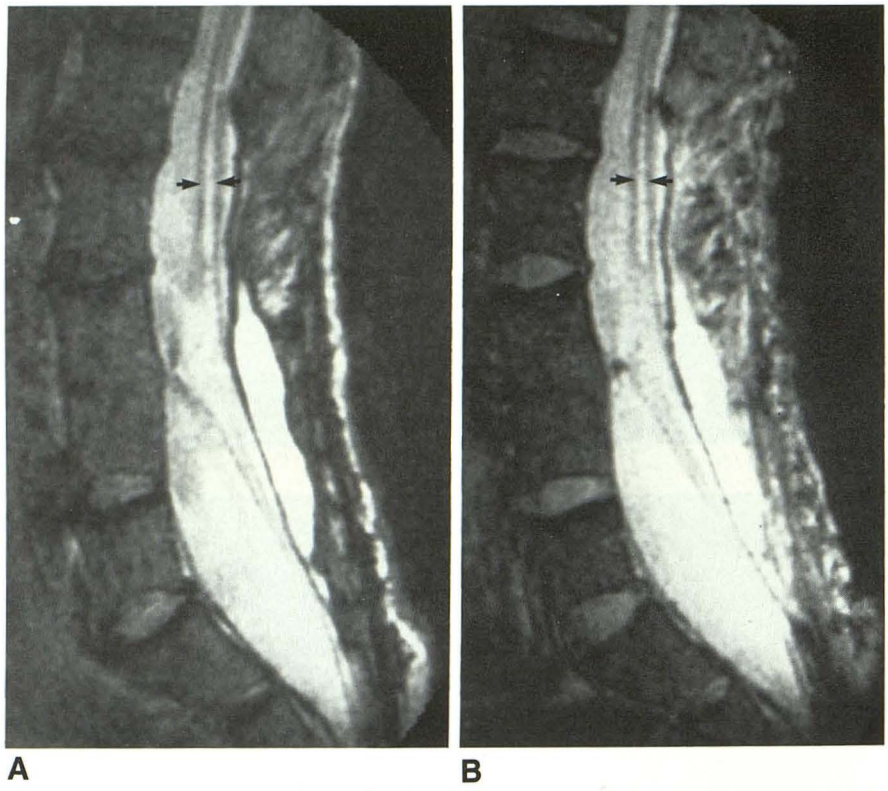

Fig. 6.—Case 19: Hydromyelia in a tethered cord in patient with postoperative diastematomyelia.

***A* and *B*, Syringohydromyelia (*arrows*) in tethered cord is seen equally well on both SE, 2000/100 (*A*), and GRE, 300/14, 10° flip angle (*B*), pulse sequences.**

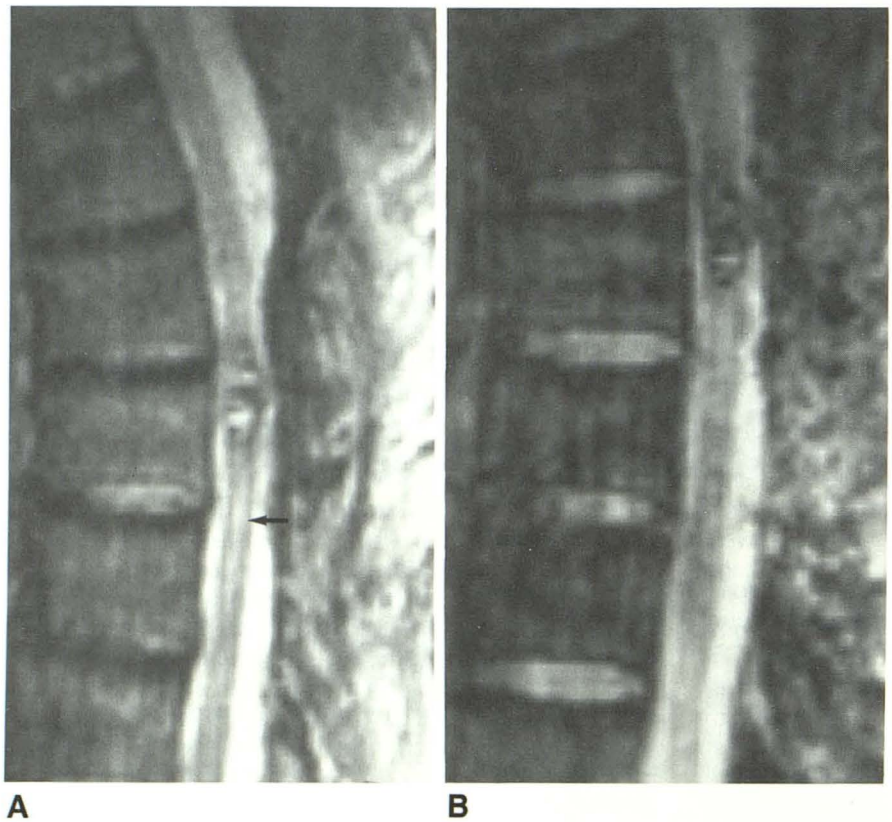

Fig. 7.—Case 16: Recurrent intramedullary hematoma in patient with presumed occult arteriovenous malformation.

***A*, T1-weighted SE image (2000/100) shows mixed signal intensity at T8 level as a result of methemoglobin and hemosiderin in both subacute/chronic hemorrhages. Truncation artifact (*arrow*).**

***B*, GRE image (300/14, 10° flip angle) shows lesion equally well. Note improved visualization of intervertebral disks secondary to lack of chemical-shift artifact. Also, truncation artifact seen on SE is not present on GRE image.**

on GRE (proton density) as a result of increased water content in these lesions. The signal intensity in proton-density imaging is related to the relative quantity of mobile protons in a particular tissue or lesion. Although the observed T2 signal and measured T2 values in a lesion also correlate positively with the amount of water present, other properties of water contribute to the T2 relaxation and signal intensities observed. These include the presence of nonwater protons such as

macromolecular proteins, the relative amounts of free vs bound water molecules, and intermolecular dipole-dipole interactions [17]. Although T2 can be measured easily [17–19], proton density is less easily quantified. On the basis of our observations, however, with respect to GRE and T2-weighted SE images, we believe there is a roughly linear relationship between signal intensities in cord lesions.

Overall, pathology was seen at least as well on GRE (proton density) as on SE sequences in 79% of the sequences. In the 21% (5/24) of cases in which the lesion was better seen on T2 (as evidenced by a "brighter" signal), all of these lesions were also easily visible on GRE imaging. In these few cases, the T2 differences between lesion and cord (image contrast) were apparently greater than the respective proton-density differences. This difference in contrast can be overcome by significantly improving the SNR, which consequently improves the contrast-to-noise ratio. The contrast-to-noise ratio is the determining factor in lesion detectability.

It became obvious early in our study that there was a remarkable difference between the anatomic quality of the images in the axial plane in favor of GRE. This was consistent with the findings of other authors [7, 15]. To understand the reasons for the superiority of GRE in the axial plane, it is important to discuss the inherent problems associated with T2-weighted SE imaging in the cervical and thoracic spine. Nongated T2-weighted images in the cervical spine produce considerable phase shifts and time-of-flight signal loss as a result of CSF pulsation, blood flow in cervical vessels, and swallowing movements. Cardiac pulsations also play a role with CSF flow directed caudally in systole and cranially during diastole. It has become clear that some sort of flow compensation is necessary to alleviate these artifacts [11–14], and many centers use either cardiac-gated spinal MR [11–14] or motion-compensating gradients on T2-weighted SE images [9, 10]. In the latter method, extra "lobes" or gradients are added in both the slice-select and read directions to refocus the additional phase shifts experienced by flowing material. Although this technique can reduce or eliminate phase errors, it cannot correct for time-of-flight errors caused by flow through the image plane. In axial imaging, the CSF motion is flowing in the slice-select direction (i.e., craniocaudad). Consequently, considerable time-of-flight effects are present in the axial plane in SE, causing degradation of the image. Our GRE sequences, on the other hand, were devoid of these time-of-flight artifacts. Time-of-flight effects can occur with the limited flip-angle technique if (1) the flip angle is large enough for T1 saturation effects to occur or (2) the TR is short enough for "steady-state" magnetization to be acquired (TR = 25–100 msec), then flow can disrupt this steady state. Both these mechanisms are avoided in the GRE protocol described here. A small flip angle (10°) is used to avoid T1 saturation and a relatively long TR (300 msec) is used to avoid a major signal contribution from transverse steady-state magnetization. In addition, the use of a short TE with a medium TR (as in our sequence, 300/14) reduces the flow-induced phase errors so that they will not contribute to motion artifacts. This results in improved diagnostic quality and explains the superior lesion/cord and cord/CSF interfaces seen on the axial GRE images (Figs. 1, 2, 3A, 3B, 4, and 8). An interesting caveat to this theory is illustrated by a case of arachnoiditis seen in Figure 9 (not among our series of 19 patients) in which the axial T2 image is equivalent to the GRE image. There are two reasons for this: (1) CSF flow and its associated artifacts are less significant in the lumbar region than in the cervical and thoracic areas and (2) intradural arachnoiditis alters CSF flow dynamics, thus diminishing CSF movement and causing fewer flow-induced artifacts.

The effects of partial-volume averaging must also be considered when comparing axial and sagittal images. Because most cord lesions extend in a craniocaudad direction along gray- and/or white-matter tracts, the lesions would be seen in the axial plane even if thick sections were used. On the

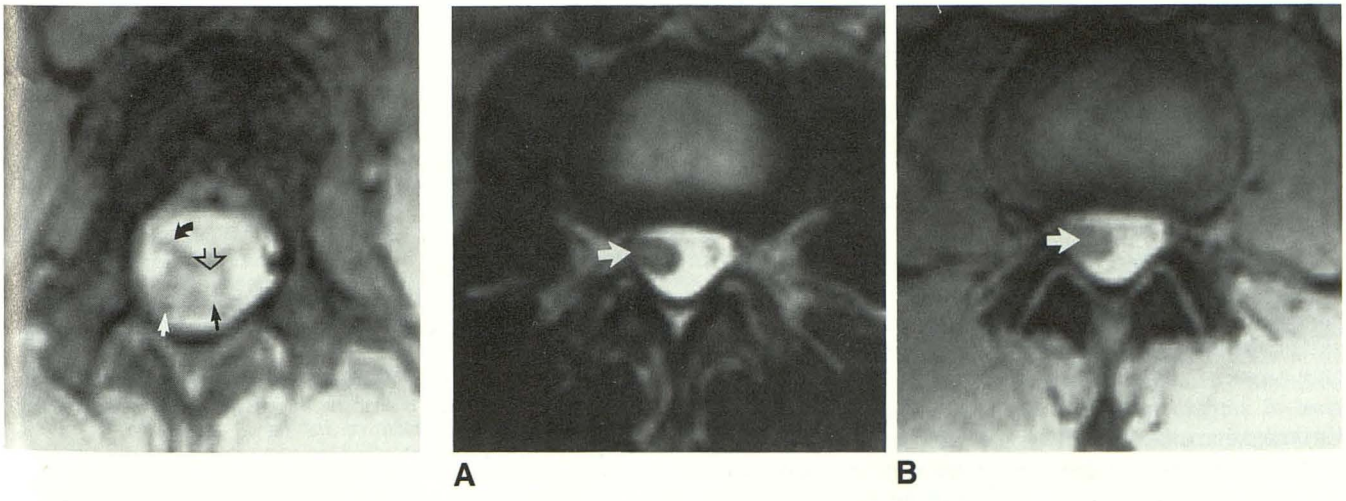

Fig. 8.—Demonstration of normal axial anatomy of lower thoracic spine by GRE. Note excellent definition of central gray matter including dorsal (*solid straight black arrow*) and ventral (*open arrow*) gray columns. Ventral roots are well visualized (*curved arrow*). Dorsal white matter (*white arrow*) can be seen easily.

Fig. 9.—Arachnoiditis of lumbar spine at L2–L3 level.

***A*, Axial T2-weighted SE image, 2000/100 (*A*), and GRE image, 300/14, 10° flip angle (*B*), are equal in quality. This is believed to result from sluggish CSF flow in lumbar spine, which is made especially stagnant in this case of arachnoiditis. Note clumped nerve roots (*arrows*), which adhere to right side of thecal sac. Excellent anatomic detail is achieved in both sequences.**

other hand, sagittal SE or GRE imaging is often plagued by partial-volume averaging of the cord with the hyperintense CSF, especially if thick cuts are used. For these reasons, small lesions could be missed by either technique in the sagittal plane.

We believe that sagittal GRE is at least as good as T2-weighted SE for both normal anatomy and disease. This was true in 94% of sequences (14/15) (Figs. 3C, 3D, and 5–7). The direction of CSF flow is in the frequency-encoded direction with sagittal imaging, assuming that the phase-encoded direction is horizontal. There is no significant flow in the slice-select direction in this situation. Thus, there are no significant flow artifacts that cannot be removed by motion-compensating gradients. This explains why the quality of the SE images in the sagittal plane is roughly equivalent to the quality of the limited flip-angle (GRE) images.

Figure 7 illustrates two additional benefits of GRE. First, chemical shift is less apparent on GRE than on SE pulse sequences. Chemical shift is produced by spatial misregistration at interfaces between fat- and water-containing structures due to differences in their Larmor frequencies. Because fat is hypointense on GRE relative to soft tissues, the chemical shift is less visually apparent than it would be on SE, where fat is relatively hyperintense [1]. Second, truncation artifacts may also be diminished with GRE. These are caused by variable overshoot and undershoot oscillations at the abrupt transitions in signal magnitude of high-contrast boundaries. This is seen more when using 128 phase-encoding steps than 192 or 256 phase-encoding steps [20]. On GRE, the relative contrast between cord and CSF is less than on T2, making these artifacts less apparent.

On the basis of our findings, we suggest that properly optimized GRE imaging on high-field-strength systems can replace T2-weighted SE images in the spine (particularly in the cervical and thoracic areas) when a myelopathy is present and intramedullary disease is suspected. Sagittal T1, as well as sagittal and axial GRE, images can be obtained in approximately 30 min, including setup time. This protocol may alleviate many of the problems associated with long imaging times, particularly with patients who are uncomfortable or uncooperative.

A few limitations of GRE in the spine should be addressed. First, it may be more difficult to accurately stage hematomas with the GRE than with the SE technique. Although the magnetic susceptibility effects of blood play a role in staging with GRE, the proton-density effects of this technique are also important. Second, as a result of the natural fat suppression of GRE [1], fatty structures, including tumors, may be missed. Thus, we recommend that a sagittal T1 image accompany all GRE sequences in the spine to alleviate these potential pitfalls. In addition, we have found that in patients with extensive metallic wiring in the posterior elements of the spine from previous surgery, visualization of the spinal cord at the level of surgery may be inadequate. This, too, is due to ferromagnetic effects. In these patients, conventional SE sequences may be helpful. Finally, there is a limitation on the number of slices obtainable with our multisection GRE technique compared with SE. The GRE sequence acquires eight slices and covers approximately one-half the area of our routine SE sequence. Thus, it would take 7.6 min to cover the identical area compared with SE. This still represents an average of 5 min of savings compared with SE. For most cases, however, axial imaging encompassing three vertebral bodies is adequate for diagnostic purposes, and this is the approximate area covered by one GRE sequence.

In conclusion, we believe that properly optimized GRE imaging at high fields can replace SE sequences in the spine when an intramedullary lesion is suspected. The GRE sequences offer better anatomic and pathologic delineation in the axial plane, secondary to its superior contrast-to-noise ratio, and are at least equivalent to SE in the sagittal plane.

REFERENCES

1. Wehrli FW, Drayer BP. Introduction to fast-scan magnetic resonance. *BNI Q* **1987**;3(4):2–14
2. Mills TC, Ortendahl DA, Hylton NM, Crooks LE, Carlson JW, Kaufman L. Partial flip angle MR imaging. *Radiology* **1987**;162:531–539
3. Buxton RB, Edelman RR, Rosen BR, Wismer GL, Brady TJ. Contrast in rapid MR imaging: T1 and T2 weighted imaging. *J Comput Assist Tomogr* **1987**;11(1):7–16
4. Perkins TG, Wehrli FW. CSF signal enhancement in short TR gradient echo images. *Magn Reson Imaging* **1986**;4:465–467
5. Wehrli FW, Shimakawa A, Gullberg GT, MacFall JR. Time of flight MR flow imaging: selective saturation recovery with gradient refocusing. *Radiology* **1986**;160:781–785
6. Enzmann DR, Rubin JB. Cervical spine: MR imaging with a partial flip angle, gradient-refocused pulse sequence. Part I: General considerations and disk disease. *Radiology* **1988**;166:467–472
7. Hedberg MC, Drayer BP, Flom RA, Hodak JA, Bird CR. Gradient echo (GRASS) MR imaging in cervical radiculopathy. *AJNR* **1988**;9:145–151, *AJR* **1988**;150:683–689
8. Watanabe AT, Teitelbaum GP, Bradley WG, Whitemore AR. Comparison of gradient echo and spin echo transaxial imaging of the lumbar spine. Presented at the annual meeting of the American Society of Neuroradiology, Chicago, May **1988**
9. Pattany PM, Phillips JJ, Chiu LC, et al. Motion artifact suppression technique (MAST) for MR imaging. *J Comput Assist Tomogr* **1987**;11(3):369–377
10. Quencer RM, Hinks RS, Pattany PH, Horen M, Post MJD. Improved MR imaging of the brain by using compensating gradients to suppress motion-induced artifacts. *AJNR* **1988**;9:431–438, *AJR* **1988**;151(1):163–170
11. Enzmann DR, Rubin JB, Wright A. Use of cerebrospinal fluid gating to improve T2 weighted images. Part I. The spinal cord. *Radiology* **1987**;162:763–767
12. Rubin JB, Enzmann DR, Wright A. CSF-gated MR imaging of the spine: theory and clinical implementation. *Radiology* **1987**;163:784–792
13. Rubin JB, Enzmann DR. Imaging of spinal CSF pulsation by 2DFT MR: significance during clinical imaging. *AJNR* **1987**;8:297–306, *AJR* **1987**;148:973–982
14. Rubin JB, Enzmann DR. Harmonic modulation of proton MR precessional phase by pulsatile motion: origin of spinal CSF flow phenomena. *AJNR* **1987**;8:307–318, *AJR* **1987**;148:983–994
15. Enzmann DR, Rubin JB. Cervical spine: MR imaging with a partial flip angle, gradient-refocused pulse sequence. Part II. Spinal cord disease. *Radiology* **1988**;166:473–478
16. Holtas S, Stahlberg F, Cronquist S, Larsson EM. Low flip angle MR imaging of the cervical spine. Presented at the annual meeting of the American Society of Neuroradiology, Chicago, May **1988**
17. Thomas SR, Dixon RL, eds. *NMR in medicine: the instrumentation and clinical applications.* New York: American Institute of Physics, **1986**:201–213, 224–227
18. Darwin RH, Drayer BP, Riederer SJ, Wang HZ, MacFall JR. T2 estimates in healthy and diseased brain tissue: a comparison using various MR pulse sequences. *Radiology* **1986**;160:375–381
19. Bottomley PA, Foster TH, Argersinger RE, Pfeifer LM. *A review of normal tissue hydrogen NMR relaxation times and relaxation mechanisms from 1–100 MHz: dependence on tissue type, NMR frequency, temperature, species, excision, and age*: General Electric technical information series. Milwaukee, WI: General Electric, **1984**:1–34
20. Levy LM, DiChiro G, Brooks RA, Dwyer AJ, Wener L, Frank J. Spinal cord artifacts from truncation errors during MR imaging. *Radiology* **1988**;166:479–483